etadata, citation and similar papers at core.ac.uk

Accepted Manuscript

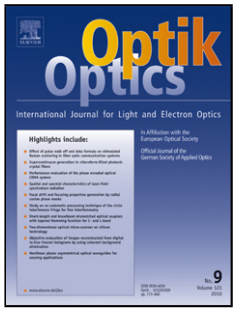

Title: On the estimation of face recognition system performance using image variability information

Authors: Muhammad Aurangzeb Khan, Costas Xydeas, Hassan Ahmed

PII: S0030-4026(17)30206-1
DOI: http://dx.doi.org/doi:10.1016/j.ijleo.2017.02.063
Reference: IJLEO 58879

To appear in:

Received date: 8-8-2016
Revised date: 17-2-2017
Accepted date: 17-2-2017

Please cite this article as: Muhammad Aurangzeb Khan, Costas Xydeas, Hassan Ahmed, On the estimation of face recognition system performance using image variability information, Optik - International Journal for Light and Electron Optics http://dx.doi.org/10.1016/j.ijleo.2017.02.063

This is a PDF file of an unedited manuscript that has been accepted for publication. As a service to our customers we are providing this early version of the manuscript. The manuscript will undergo copyediting, typesetting, and review of the resulting proof before it is published in its final form. Please note that during the production process errors may be discovered which could affect the content, and all legal disclaimers that apply to the journal pertain.

ACCEPTED MANUSCRIPT

On the Estimation of Face Recognition System Performance using Image Variability Information

Muhammad Aurangzeb Khan[a], Costas Xydeas[b], Hassan Ahmed[c]

School of Computing and Communication
Infolab21, Lancaster University, Lancaster, LA1 4WA, United Kingdom
[a]aurangzebniazi@gmail.com
[b]c.xydeas@lancaster.ac.uk,
[c]h.ahmed@lancaster.ac.uk

[1]**Corresponiding Author** is currently working as Assistant Professor in Electrical Engineering Department at COMSATS Institute of Information Technology, Islamabad, 44000, Pakistan. Phone: +923355211600 and this work is a part of authors' PhD research done at Lancater University, United Kingdom.

Abstract

The type and amount of variation that exists among images in facial image datasets significantly affects Face Recognition System Performance (FRSP). This points towards the development of an appropriate image Variability Measure (VM), as applied to face-type image datasets. Given VM, modeling of the relationship that exists between the image variability characteristics of facial image datasets and expected FRSP values, can be performed.

Thus, this paper presents a novel method to quantify the overall data variability that exists in a given face image dataset. The resulting Variability Measure (VM) is then used to model FR system performance versus VM (FRSP/VM).

Note that VM takes into account both the inter- and intra-subject class correlation characteristics of an image dataset. Using eleven publically available datasets of face images and four well-known FR systems, computer simulation based experimental results showed that FRSP/VM based prediction errors are confined in the region of 0 to 10%.

Index Terms— **Face recognition (FR), Signal Variability in image face datasets, Facial Variability Measure and its relationship to FR performance.**

1. INTRODUCTION

Face Recognition (FR) has been adopted over the last three decades as the primary methodology of biometric identification and verification systems. Major characteristics which provide FR with an edge over other biometric techniques are its relatively high accuracy and non-intrusiveness nature. As a result, a plethora of face recognition techniques have been proposed; a detailed survey of such FR schemes can be found in [1-8].

Furthermore, face recognition systems usually operate in one of two modes: i) Verification (FV) and ii) Identification (FI). Face verification is a one-to-one matching process in which an input (query) face image is compared against the stored template of only one person whose identity is being claimed. On the other hand, face identification involves one-to-many comparisons between an input face image with the stored templates of a number of individuals. There are several areas where FR is applied in the form of FV or FI, e.g. in access control, surveillance, criminal justice systems, smart cards etc. see [8]. However, when employed in real life application, FR system performance is affected significantly by large intra-person and small inter-person amounts of input image variabilities which often characterize a given application domain. Furthermore, this apparent dependency of FR system performance stems from the way face images are captured. Now, and in order to test the performance of FR systems, numerous sets of face images have been created and are publically available, each using different image capture criteria and constraints [9]. Table-1 presents several well-known face image datasets, each created with its own image capture specification.

The usual image capturing conditions that count for different types of image face variability are related to:

- Illumination
- Pose
- Expression
- Makeup
- Facial attributes i.e. mustache, beard, glasses,
- Age

In addition to the above types, the amount of variability allowed per type, during image capturing, is also of importance. Consider for example the type of variability "pose" (see table 2) which can vary from 0 to ± 90 degrees. Large variations in pose can create severe visual changes between images taken of the same person, whereas, at the same time, have the potential to increase similarity between the images of different subjects. Of course in both cases FR becomes a more challenging task with adverse implications in FR system performance. This general

ACCEPTED MANUSCRIPT

dependency of FR system performance upon specific input image sets and their associated types and levels of variability is discussed in [23], see also Table 3. Here the authors employed a Tied Factor Analysis based FR algorithm and showed i) that a FR system trained and optimized using a specific type of image variability performs differently when operating over image datasets having different variability characteristics and ii) that a relationship exists between the amount of image variability and system recognition performance. This implies that, given an appropriate measure of image data variability, this relationship could be modeled which in turn suggests that the performance of a given FR system could be predicted for any given input face dataset without the need to perform FR experimentation.

Thus the ability to i) measure image face data variability VM and ii) model VM versus FR System Performance (FRSP), are important research aims. Also note that such FRSP/VM models can be used to select face recognition systems that are better suited to given applications. Furthermore, VM can be used to rank face image datasets in terms of their FR difficulty level.

To the best of our knowledge, no work has been yet reported that covers and integrates the above two FR research aims. The conceptually nearest publication [28] proposes a set of different variability measures in order to represent object class properties in object classification. In [28] proposed variability measures are based on intra-class similarities. As a consequence they can only be used with binary types of classification problems and definitely not in multiclass scenarios such as those encountered in FR.

In this paper, and for a given dataset of face images, both inter- and intra-subject dataset measures are first defined. These are subsequently combined to form a single variability measure (VM) which quantifies the overall level of image variability of a face dataset.

Furthermore the relationship is modeled, using n^{th}-degree polynomials, between the VM values of several face datasets and the corresponding face recognition rates obtained from several FR systems. Thus FRSP/VM models are derived with respect to four different face recognition (FR) systems and eleven publically available face image datasets whose VM values vary considerably.

Experimental results show that modeling FRSP in terms of VM allows relatively good performance prediction estimates. That is to say, given an unseen input face dataset and its VM value as well as a FRSP/VM model, FR system performance can be predicted reasonably well. Furthermore, this prediction capability has been also evaluated using face image datasets that are JPEG coded at four different PSNR values. Results show noise free FRSP/VM models to operate well even under noisy (coded) input image conditions.

The paper is organized as follows: Section 2 explains in detail VM formulation whereas Section 3 describes the experimental set up used to produce computer simulation results. These results are then presented and discussed in the second part of Section 3. Concluding remarks are given in Section 4.

2. VARIABILITY MEASURE (VM)

The proposed overall variability measure VM of an image dataset is made of two components i.e. an inter- and an intra-Subject Class, denoted as VM-interSC and VM-intraSC respectively.

2.1 VM-intra- and VM-inter-Subject Class Components

VM-intra- and VM-inter-Subject Class are basically measures of similarity among images belonging to same subject class and images from different classes, respectively. In this paper, the Normalized Cross Correlation (NCC) [29] is used as a similarity measure between two given face images A and B. In VM-intraSC, NCC is calculated among all the available images of each subject, whereas in VM-interSC, NCC is calculated among all images of one subject with respect to all images of all other subjects.

*2.1.1 **VM-intraSC***

First step to calculate VM-intraSc is to create a $P \times Q$ dimensional matrix $\widehat{\mathbf{C}}$ of of NCC values, see Eq. 1:

$$\hat{\mathbf{C}}(\boldsymbol{p},\boldsymbol{q}) = \begin{bmatrix} \vartheta_{12}^{1} & \vartheta_{12}^{2} & \cdots & \vartheta_{12}^{M} \\ \vartheta_{13}^{1} & \vartheta_{13}^{2} & \cdots & \vartheta_{13}^{M} \\ \vdots & \vdots & \vdots & \vdots \\ \vartheta_{1N}^{1} & \vartheta_{1N}^{2} & \cdots & \vartheta_{1N}^{M} \\ \vartheta_{23}^{1} & \vartheta_{23}^{2} & \cdots & \vartheta_{23}^{M} \\ \vartheta_{24}^{1} & \vartheta_{24}^{2} & \cdots & \vartheta_{24}^{M} \\ \vdots & \vdots & \vdots & \vdots \\ \vartheta_{2N}^{1} & \vartheta_{2N}^{2} & \cdots & \vartheta_{2N}^{M} \\ \vdots & \vdots & \vdots & \vdots \\ \vartheta_{(N-2)(N-1)}^{1} & \vartheta_{(N-2)(N-1)}^{2} & \cdots & \vartheta_{(N-2)(N-1)}^{M} \\ \vartheta_{(N-2)(N)}^{1} & \vartheta_{(N-2)(N)}^{2} & \cdots & \vartheta_{(N-2)(N)}^{M} \\ \vartheta_{(N-1)N}^{1} & \vartheta_{(N-1)N}^{2} & \cdots & \vartheta_{(N-1)N}^{M} \end{bmatrix}. \quad (1)$$

Here the number of columns P is equal to the number of subjects M whereas the number of rows Q is equal to $\frac{N(N-1)}{2}$; N is the number of images per subject in a particular face dataset. Each element ϑ_{nk}^{m} of $\widehat{\mathbf{C}}(\boldsymbol{p},\boldsymbol{q})$ represents the maximum value of an array $\{\boldsymbol{\gamma}_{nk}^{m}(u,v)\}$ that contains all NCC normalized cross correlation values $\boldsymbol{\gamma}_{nk}^{m}(u,v)$ formed between images I_{n}^{m} and I_{k}^{m} of subject m. i.e.

$$\vartheta_{nk}^{m} = maximum\ element\{\boldsymbol{\gamma}_{nk}^{m}(u,v)\}, \quad (2)$$

ACCEPTED MANUSCRIPT

Furthermore

$$\boldsymbol{\gamma}_{nk}^{m}(u,v) = \frac{\sum_{x,y}\left[\mathbf{I}_n^m(x,y)-\overline{\mathbf{I}_n^m}\right]\left[\mathbf{I}_k^m(x-u,y-v)-\overline{\mathbf{I}_k^m}\right]}{\sqrt{\sum_{x,y}\left[\mathbf{I}_l^m(x,y)-\overline{\mathbf{I}_l^m}\right]^2\sum_{x,y}\left[\mathbf{I}_k^m(x-u,y-v)-\overline{\mathbf{I}_k^m}\right]^2}}. \quad (3)$$

where x and y are pixel coordinates, and u and v refer to the shift at which a NCC value is calculated. Moreover, $\overline{\mathrm{I}_n^m}$ and $\overline{\mathrm{I}_k^m}$ are the means of the overlapped regions of the two images.

Once, $\hat{\mathbf{C}}$ is formed for a specific dataset, VM-intraSc = $\widehat{\emptyset}$ is calculated as

$$\widehat{\emptyset} = \hat{\mu} \times \hat{\sigma}^2,$$

where

$$\hat{\mu} = \frac{1}{(P\times Q)}\sum_{p=1}^{P}\sum_{q=1}^{Q}\hat{C}(p,q), \quad (4)$$

and

$$\hat{\sigma}^2 = \frac{1}{(P\times Q)-1}\sum_{p=1}^{P}\sum_{q=1}^{Q}(\hat{C}(p,q)-\hat{\mu})^2.$$

In Eq. 4, higher values of mean $\hat{\mu}$ represent larger similarity or lesser variation among the images of each subject. Furthermore larger variance $\hat{\sigma}^2$ values correspond to wider ranges of variation about the mean for the images of each subject. Also note that both $\hat{\mu}$ and $\hat{\sigma}^2$ are related to the number of images N used per subject. Thus when N is relatively large so that subject images vary smoothly, even when the overall variation per subject is large, then relatively large VM-intraSC $\widehat{\emptyset}$ values are produced.

In order to further consider the above statements and the relationship between $\hat{\mathbf{C}}(\boldsymbol{p},\boldsymbol{q})$ values and input image dataset characteristics, the following two experiments were performed. Both involved Part-2 of the FEI face dataset [16]. FEI is a publically available face dataset that comes in four different parts. Each part contains 50 subjects with 14 color images per subject. 10 out of these 14 images cover smoothly a rotation profile of up to 180°, whereas the remaining 4 images contain illumination and expression variation. In the first experiment, two matrices $\hat{\mathbf{C}}_1$ and $\hat{\mathbf{C}}_2$ are formed from two different FEI Part-2 subsets. The first subset contains smooth rotational variations and comprises of all 10 images per subject. The second subset contains only 3 images per subject taken with subject rotations 0°, 90° and 180°. In Fig.1, two normalized histograms corresponding to $\hat{\mathrm{C}}_1$ and $\hat{\mathrm{C}}_2$ values are shown, respectively. The histogram corresponding to the dataset having smooth pose variations from 0° to 180° (Fig.1 (a)) covers a larger range of NCC values and hence yields a larger intra-subject measure value $\widehat{\emptyset}_1 = 0.0119$, as compared to $\widehat{\emptyset}_2 = 0.0061$ of the second dataset see Fig.1 (b).

In the second experiment, VM-intraSC values are calculated for four different datasets named as DS1, DS2, DS3 and DS4 to produce the curve shown in Fig.2. All four datasets used here are different from each other with respect to number of images used per subject and pose variation between successive images.

In particular DS1 dataset contains three images per person with approximate of 0^{o}, 90^{o} and 180^{o} rotations respectively, DS2 comprises of four images per person with approximate rotations at 0^{o}, 60^{o}, 120^{o} and 180^{o}, respectively, DS3 contains five images per subject with approximate rotations at 0^{o}, 45^{o}, 90^{o}, 135^{o} and 180^{o}, respectively and finally DS4 contains all the ten images per subject. It is obvious from Fig.2 that an increase in number of images per subject used to cover a large range of image rotational type of variability i.e. 0^{o} to 180^{o}, increases the level of similarity between subject images and as a consequence increases VM-intraSC $\widehat{\emptyset}$.

*2.1.2 **VM-interSC***

As discussed in the previous section, quantifying intra-subject variation alone cannot adequately represent an overall VM, since inter-subject dataset properties are also equally important and should be taken into account.

In particular and in order to successfully distinguish between images of different subjects, there must be large variations among these images. Thus to quantify such inter-subject variability, another matrix $\check{\mathbf{C}}$ (see Eq. 5) can be created that contains the Normalized Cross-Correlation values of all images of one subject cross-correlated and all the images of all other subjects.

$$\check{\mathbf{C}} = \begin{bmatrix} \boldsymbol{C}^{12} & \mathbf{0} & \mathbf{0} & & \mathbf{0} \\ \boldsymbol{C}^{13} & \boldsymbol{C}^{23} & \mathbf{0} & \cdots & \mathbf{0} \\ \boldsymbol{C}^{14} & \boldsymbol{C}^{24} & \boldsymbol{C}^{34} & & \mathbf{0} \\ \vdots & \vdots & \vdots & \ddots & \vdots \\ \boldsymbol{C}^{1M} & \boldsymbol{C}^{2M} & \boldsymbol{C}^{3M} & \cdots & \boldsymbol{C}^{(M-1)M} \end{bmatrix},$$

and

$$\boldsymbol{C}^{ml} = \begin{bmatrix} \vartheta_{11}^{ml} \\ \vartheta_{12}^{ml} \\ \vdots \\ \vartheta_{1N}^{ml} \\ \vartheta_{21}^{ml} \\ \vartheta_{22}^{ml} \\ \vdots \\ \vartheta_{2N}^{ml} \\ \vdots \\ \vartheta_{N1}^{ml} \\ \vdots \\ \vartheta_{NN}^{ml} \end{bmatrix}, \quad \text{with } m < l. \quad (5)$$

In Eq. 5 ϑ_{nk}^{ml} is the maximum NCC between nth image of subject m i.e. I_n^m, and kth image of subject l i.e. I_k^l. The

ACCEPTED MANUSCRIPT

value of ϑ_{nk}^{ml} is calculated in the same way as given in Eq. 2 and Eq. 3. The order of matrix $\check{\mathbf{C}}$ is $G \times H$ where the number of rows G is equal to $(M-1) \times N^2$ and number of columns are equal to $M-1$. Once the matrix $\check{\mathbf{C}}$ is obtained, it is used to form VM-interSC ($\breve{\emptyset}$) as given in Eq. 4. The corresponding $\breve{\mu}$ and $\breve{\sigma}^2$ are calculated using only elements present in the lower triangle of the matrix $\check{\mathbf{C}}$.

In case of inter-subject variability, a face dataset with large variations among the images of different subjects, yields smaller NCC values which in turn result in smaller mean and variance values and hence in a relatively small $\breve{\emptyset}$ value.

Thus a dataset of face images with large inter-class variations (i.e. small VM-interSC $\breve{\emptyset}$ value) and small intra-class variation (i.e. large intra-SC $\hat{\emptyset}$ value) should exhibit high classification performance. It is therefore expected that a face image dataset that is characterized by the following condition:

$$\breve{\emptyset} \ll \hat{\emptyset}, \tag{6}$$

should produce relatively high classification results. Consider for example, the proposed VM-interSCs for two subsets used in the first of the previously mentioned two experiments. Their corresponding VM-interSC values are $\breve{\emptyset}_1 = 0.0068$ and $\breve{\emptyset}_2 = 0.0071$, respectively and hence the first subset with $\breve{\emptyset}_1 < \hat{\emptyset}_1$ can yield better recognition performance for any FR system as compared to second subset where $\breve{\emptyset}_2 > \hat{\emptyset}_2$.

2.2 Variability Measure (VM)

VM-intraSC and VM-interSC, as defined in the previous section, are combined to form a single image dataset variability measure (VM). That is:

$$\text{VM} = \emptyset = \hat{\emptyset} \times \sqrt{\hat{\emptyset}^2 - \breve{\emptyset}^2}, \quad \text{for} \quad \hat{\emptyset} > \breve{\emptyset} \tag{7}$$

$\breve{\emptyset}$ and $\hat{\emptyset}$ are the previously defined inter- and intra-subject measures, respectively. In this product based formulation, $\hat{\emptyset}$ is included to scale the above square root based difference and is in this way allow VM to distinguish between datasets having same or very similar $\sqrt{\hat{\emptyset}^2 - \breve{\emptyset}^2}$ values but different VM-intraSC values. In this case the dataset with a higher VM-intraSC value will yields a larger VM value.

Moreover, the above VM formulation produces only $\emptyset$ values for datasets satisfying the $\hat{\emptyset} > \breve{\emptyset}$ condition. Datasets which are characterized by the $\hat{\emptyset} \leq \breve{\emptyset}$, classification adverse condition, are marked as inappropriate and their generation should be carefully reconsidered.

3. EXPERIMENTATION & DISCUSSION

In order to investigate the effectiveness and validity of the proposed face image variability measure VM a number of experiments have been performed. These are based on i) eleven different and publically available datasets of face images and ii) four different face recognition (FR) systems. Firstly in this section, the datasets and FR systems employed are briefly introduced, followed by the experimental setup, computer simulation results and an associated discussion.

3.1 Datasets of face images

The following image datasets have been used in our experiments:

i. AT&T Face dataset [10]
This contains a total of 400 grayscale images; that is ten images for each of 40 different subjects. Image size is restricted to 112×92 pixels. Furthermore the 10 images of each subject differ from each other with respect to lighting conditions, facial expression and facial details.

ii. IMM Face Dataset [11]
IMM consists of 240 annotated images (6 images per person). Each image is 640×480 pixels in size and comes with 58 hand labeled shape points which outline face contours. The images of each subject vary in lighting, pose and facial expression. From the available 40 subjects, 37 are represented by RGB images whereas the remaining three subjects are represented by grayscale images.

iii. The Extended Yale Cropped Face Dataset [12]
The original extended Yale Face Dataset B [12] contains 16128 images of 28 persons, under 9 poses and 64 illumination conditions. In this paper a cropped version of the dataset, as reported in [30], has been used. This version contains 2242 grayscale images of 38 subjects with images being manually aligned, cropped and then resized to 168×192 pixels.

iv. Georgia Tech. Face Dataset [13]
This contains images taken from 50 different subjects. There are 15 RGB images per subject and vary in size, facial expression, illumination and rotation. The average face size is 150×150 pixels.

v. Stirling Face Dataset [14]
The Stirling face dataset contains the 312 images of 35 subjects (18 female, 17 male). These are mono-

ACCEPTED MANUSCRIPT

chrome images with 269×369 pixels spatial resolution and vary in pose and facial expression.

vi. Indian Face Dataset [15]
This database contains the images of 55 subjects (22 female, 33 male) and features eleven different poses per individual. In addition to pose variability, images with four emotions i.e. neutral, smile, laughter, sad/disgust, are also included for every individual. The size of each image is 640×480 pixels, with 256 grey levels per pixel.

This Indian dataset has been divided further into two i.e. a male and a female subset, which in turn are two of the 11 datasets employed during experimentation.

vii. FEI Face Dataset [16]
The FEI face dataset comes in four different subsets which have been used as part of the previously mention experimentation involving 11 subsets. Each subset contains 50 subjects with 14 RGB images per subject. Furthermore 10 out of these 14 images cover smoothly a rotation profile of up to 180°, whereas the remaining 4 contain variations in illumination and expression. FEI image size is 640×480 pixels.

Finally note that all dataset images are manually cropped in order to remove any background information. Some cropped sample images are shown in Fig.3 along with their corresponding original images.

3.2 Face Recognition (FR) Systems

Four different face recognition (FR) systems have been employed in order to experimentally determine VM modeling performance. Note that as i) the purpose of this work is not to provide a comparison between different face recognition system and ii) we are not offering any state-of-the-art face recognition system solutions, we have chosen four appearance based face recognition system formulations that are relatively simple and easily implementable. Their brief description is given below:

i. Eigenfaces:
The "Eigenfaces", approach has been introduced by Turk and Pentland [31], is one of the most thoroughly investigated FR techniques [32-34].
Eigenfaces are the eigenvectors that characterize variation across different face images in a training dataset. Each N-dimensional face image is a linear combination of these eigenvectors and can be best approximated using only a few M ($M \ll N$) that is 'the best' eigenvectors or principal components (PCs), in terms of the largest corresponding eigenvalues containing P percent of overall training face data variation. Normally, P is kept in the range of $90 - 95$ and is set here as $P = 95$. Furthermore face images from both training and testing datasets are projected into a subspace, the so called "facespace", which is defined by the above M Eigenfaces. Thus recognition is performed in the facespace by calculating the distance between known points derived from training images and unknown points representing testing images.

ii. Fisherfaces:
The second face recognition technique, that has been used in this work, is the well-known "Fisherfaces". Fisherfaces, as proposed by [35], is based on a two-stage strategy. In the first stage, a principal component analysis (PCA) is performed in, the same way as in Eigenfaces, to reduce the face image dimension. A linear discrimination analysis (LDA) follows that extracts discriminative information from the reduced dimensionality data. Note that LDA is maximizing between-class variation and at the same time is minimizing within-class variation. The original Fisherfaces approach has been heavily investigated and modified to produce several different face recognition systems [36-39].

iii. PCA + Multi-Class SVM:
In this case, PCA is used as a preprocessing step for dimensionality reduction and then the well-known Support Vector Machine (SVM) is used in a multi-class mode to classify these dimensionality reduced vectors.
SVM, originally introduced by Vapnik and Cortes [40] for binary classification, is normally extended and thus adapted to multi-class problems by using two basic strategies i.e., i) One-versus-One and ii) One-versus-All [41]. The basic difference in these strategies is the number of classifiers trained. In the One-versus-One approach, one classifier designed for each pair of classes. Thus for N classes, $\frac{N(N-1)}{2}$ classifiers are needed. During classification and for every test sample, each classifier votes for one of the two classes and the class with maximum number of votes is selected. In the One-versus-All case, one classifier per class is built and trained to classify between each class and rest of the classes, in this way only N classifiers are designed. In this paper, the One-versus-All approach has been used as it is computationally less expensive than the alternative One-versus-One scheme.
Furthermore SVM works on the principle of finding an optimal linear hyperplane that separates two classes from each other. Note that in most real-world applications linear separation is not feasible, and SVM is modified to act as a non-linear classifier using a kernel technique. Here kernels transform data into a higher dimensional space where linear classification is feasible.

ACCEPTED MANUSCRIPT

In this work a radial basis function (RBF) kernel has been used. This is effectively based on a Gaussian kernel and is dependent on two parameters, one is the so called kernel parameter $K\sigma$ whereas the other is known as the penalty factor KC. Note that for each dataset, the values of these parameters were selected to maximize recognition performance.

iv. Normalized Cross-Correlation:
This final face recognition technique operates on the basis of maximum Normalized Cross-Correlation (NCC) values derived between input test face image and training images. Notice that prior to NCC calculation, both test and training images are normalized to images having zero mean and unit variance.

3.3 Results and Discussion

The effectiveness of using the VM value of a certain face image dataset to predict the performance of FR systems, operating on the same image dataset, is considered in this section. To this end the test method, whose architecture is shown in Fig. 4, has been deployed. Here experimentation includs two parts.

The first part involves i) computation of VM for all available datasets and ii) actual face recognition performance of the above four listed FR systems. Estimates from (i) and (ii) provide prediction error range values. Note that for all datasets, FR systems are separately designed to deliver maximum performance.

Furthermore the performance of each FR system is evaluated using the k-fold approach; k is equal to the number of images per subject in a particular face image dataset and each fold contains one image per subject. For a k-fold cross validation test, k experiments are performed and in each experimental run, (k-1)-folds are used to train the classifier whereas the remaining fold is used for testing. At the end, an average recognition rate is calculated across all folds. Recognition performance versus VM curves for all FR systems are shown in Fig.5. Curve points are obtained from different face image datasets. A general increasing trend in all curves shows that system classification performance improves with increasing variability measure (VM) values. Note however that this relationship is not monotonic.

The second part of experimentation is related to predictor block shown in Fig. 4. The predictor involves a polynomial based model that takes VM values corresponding to some face image dataset and yields predicted recognition performance of a given FR system. Here the polynomial model, that can best fit this relationship, is selected on the basis of two 'goodness of fit' parameters, that is R-squared (R^2) and adjusted R-squared ($\overline{R^2}$) .

R^2 which is generally known as coefficient of determination, is defined as the ratio of the sum of squares due to regression, with respect to the total sum of squares. $\overline{R^2}$ is a modified version of R^2 which has been adjusted with respect to the number of model variables [42].

ACCEPTED MANUSCRIPT

Note that the value of R^2 increases with an increase in the number of terms, even if new terms have no significance in improving the model. On the other hand $\overline{R^2}$, even being positively biased, is more consistent and only increases if a new term improves the model. Thus modeling improves with both R^2 and $\overline{R^2}$ assuming higher values and also with the difference between the two parameters being minimum [43].

Fig.6 shows R^2 and $\overline{R^2}$ values against different polynomial degrees for all recognition schemes. Note that as the polynomial degree (d) is increased more than $d = 2$, the rate of increase of $\overline{R^2}$ values gets smaller than that of R^2 and in some cases is negative, due to overfitting. Therefore $d = 2$ has been chosen for all the recognition schemes. The resulting prediction models for all FR systems are shown in Fig.7 along with their corresponding original data curves. Corresponding R^2, $\overline{R^2}$, percentage average Absolute Error (Avg. AE), and Error Range (%age) values are given in Table-4.

Avg. AE between actual recognition rate R_{Ac} and predicted recognition rate R_{Pr} is calculated as:

$$Avg.AE = \frac{1}{N}\sum_{i=1}^{N} |R_{Ac}^{i} - R_{Pr}^{i}|, \quad (9)$$

where N is the total number of face image datasets. Fig.7 graphs and Table-4 data show that 2nd-degree polynomials provides a relatively good fit to the available data and suggest that a useful relationship always exists between data variability VM and face recognition system performance (FRSP).

The mathematical equations of the models developed for the previously discussed four FR systems are given in Appendix A.

Next and given the VM values of "different" FR image face datasets, the effectiveness of this FR system performance prediction approach is of course of interest. Now and since in real life FR applications some type of compression coding may be used prior to FR, experiments were conducted with the previously employed 11 datasets being corrupted with coding noise introduced at different PSNR levels.

Furthermore the introduction of noise in input sample images can answer an important question i.e. how does the above derived FR system performance as related to VM models, which have been derived using noise-free image data, is affected by noisy input data? Or alternatively does the relationship defined between VM and system recognition performance also holds for noisy images?

Thus experimentation was performed using JPEG coded face image datasets and according to the experimental set up of Fig. 8. This type of coding introduces a "block" type of noise/distortion. Note that for simplicity only the Fisherfaces FR approach was employed and JPEG coding noise was adjusted at the four average PSNR values of $55.57, 33.48, 26.86, 23.98$ dbs.

In Fig. 9 actual VM and recognition rate values are obtained using noisy input data at different PSNR values. Notice that a similar increasing trend in VM and recognition performance values is observed in these curves, as in the case of noise free image based experimentation, see Fig. 5.

Moreover, curves are now shifted towards the bottom-left corner as the noise level increases. Thus a downward shift indicates that coding noise is suppressing facial variation across different subjects, which in turn causes a decrease in recognition performance whereas a left shift shows that a simultaneous decrease in VM has

In addition, models derived from clean/un-coded data were employed to predict the recognition performance of systems operating on JPEG coded image data. The histograms of absolute prediction error (%age) for all the datasets and also percentage values of Average Absolute Errors (Avg. AE) corresponding to each average PSNR level are shown in Fig. 10 and Table-5, respectively. It is obvious from these values that in spite of introducing moderate image quality coding degradation in the input face images, model error ranges are approximately the same with those derived from noise-free data. This is indicative of the relative robustness of the proposed FRSP/VM system performance relationship with respect to coding distortion.

4. CONCLUSION

This paper investigated the modeling of FR system performance in terms of the signal variability measure derived from input image datasets. Thus a new variability measure (VM) that characterizes overall image face data variability has been defined and used over a number of well-known image datasets. In addition, relationships between such VM values and the performance of four conventional FR systems have been determined and modeled using second order polynomials. Note that the proposed VM measure takes into account both inter and intra correlation image dataset characteristics.

Thus computer simulation results involving 11 publically available face image datasets show FRSP/VM prediction errors of less than 10%, for all four FR systems, and Avg. AE values across FR systems in the range of 3.27% and 5.47%. An increase in the number of available image datasets should further improve modeling accuracy. Note: free availability of public face images datasets and complexity involved in recognition process are two major factors in using only 11 face images datasets in modeling process.

Furthermore, the prediction accuracy of the above noise-free FRSP/VM models has been also assessed using noisy i.e. JPEG coded, image data at different PSNR

ACCEPTED MANUSCRIPT

values. Prediction errors (i.e. Avg. AE) corresponding to face image data coded at different PSNR values shown that these noise-free FRSP/VM models kept their prediction accuracy to approximately the same level with that produced by noise-free input data. Moreover FRSP/VM curves show the same increasing trend as those of noise-free data. This suggests that any deterioration in recognition performance, due to input image noise, is counterbalanced by VM reductions so that the general FRSP/VM relationship is maintained.

REFERENCES

[1] Patel, Riddhi, and Shruti B. Yagnik. "A Literature Survey on Face Recognition Techniques." *International Journal of Computer Trends and Technology (IJCTT)* 5.4 (2013): 189-194.

[2] Zhao, Wenyi, and Rama Chellappa. eds. "Face Processing: Advanced Modeling and Methods: Advanced Modeling and Methods." *Academic Press*, 2011.

[3] Li, Z. Stan, and Anil K. Jain. "Handbook of face recognition." *2nd Edition springer*, 2011.

[4] Chellappa, Rama, Charles L. Wilson, and Saad Sirohey. "Human and machine recognition of faces: A survey." *Proceedings of the IEEE* 83.5 (1995): 705-741.

[5] Lu, Yongzhong, Jingli Zhou, and Shengsheng Yu. "A survey of face detection, extraction and recognition." *Computing and informatics* 22.2 (2003): 163-195.

[6] Tolba, A. S., A. H. El-Baz, and A. A. El-Harby. "Face Recognition: A Literature Review." *International Journal of Signal Processing* 2.2 (2006).

[7] Meethongjan, Kittikhun, and Dzulkifli Mohamad. "A Summary of literature review: Face Recognition." (2007).

[8] Jafri, Rabia, and Hamid R. Arabnia. "A Survey of Face Recognition Techniques." *JIPS* 5.2 (2009): 41-68.

[9] Abate, Andrea F., et al. "2D and 3D face recognition: A survey." *Pattern Recognition Letters* 28.14 (2007): 1885-1906.

[10] AT&T face database, AT&T Laboratories, Cambridge, U.K, [Online] Available: http://www.cl.cam.ac.uk/research/dtg/attarchive/facedatabase.html

[11] M.M. Nordstrøm, M. Larsen, J. Sierakowski, and M.B. Stegmann, "The imm face database-an annotated dataset of 240 face images," *Informatics and Mathematical Modeling*, 2004.

[12] A. Georghiades, D. Kriegman, and P. Belhumeur, "From Few to Many: Generative Models for Recognition under Variable Pose and Illumination," IEEE Trans. Pattern Analysis and Machine Intelligence, vol. 40, pp. 643-660, 2001.

[13] Georgia Tech Face Database, ftp://ftp.ee.gatech.edu/pub/users/hayes/facedb/.

[14] Stirling face database, [Online] Available: http://pics.stir.ac.uk

[15] Vidit Jain, Amitabha Mukherjee. The Indian Face Database.

http://vis-www.cs.umass.edu/~vidit/IndianFaceDatabase/ , 2002.

[16] FEI Face Database, http://fei.edu.br/~cet/facedatabase.html.

[17] K Messer, J Matas, J Kittler, J Luettin, and G maitre. Xm2vtsdb: The extended m2vts database. In Second International Conference of Audio and Video-based Biometric Person Authentication, March 1999

[18] Daniel B Graham and Nigel M Allinson, "Characterizing Virtual Eigen signatures for General Purpose Face Recognition," Face Recognition: From Theory to Applications, NATO ASI Series F, Computer and Systems Sciences, Vol. 163. H. Wechsler, P. J. Phillips, V. Bruce, F. Fogelman-Soulie and T. S. Huang (eds), pp 446-456, 1998.

[19] Bern Univ. Face Database, ftp://iamftp.unibe.ch/pub/Images/FaceImages/, 2002.

[20] R. Singh, M. Vatsa, A. Ross, A. Noore, A mosaicing scheme for pose-invariant face recognition, IEEE Trans. Syst., Man, Cybern. B, Cybern. 37 (5) (2007) 1212–1225

[21] D. Beymer, T. Poggio, Face recognition from one example view, in: Proceedings of the International Conference on Computer Vision, 1995, pp. 500–507.

[22] Shaokang Chen and Brian C. Lovell, "Illumination and Expression Invariant Face Recognition with One Sample Image", ICPR, pp.300-303, 17th International Conference on Pattern Recognition (ICPR' 04) – Volume 1, 2004

[23] S.J.D. Prince, J. Warrell, J.H. Elder, F.M. Felisberti, Tied factor analysis for face recognition across large pose differences, IEEE Trans. Pattern Anal. Mach. Intell. 30 (6) (2008) 970–984.

[24] P.J. Phillips, H. Wechsler, J. Huang, P. Rauss, The FERET database and evaluation procedure for face recognition algorithms, Image Vision Comput. 16 (5) (1998) 295–306.

[25] T. Sim, S. Baker, and M. Bsat, "The CMU pose, illumination, and expression database," IEEE Trans. Pattern Anal. Mach. Intell., vol. 25, no. 12, pp. 1615-1618, Dec. 2003.

ACCEPTED MANUSCRIPT

[26] X. Chai, S. Shan, X. Chen, and W. Gao, "Locally Linear Regression for Pose-Invariant Face Recognition," IEEE Trans. Image Processing, vol. 16, pp. 1716-1725, 2007.

[27] T. Kanade and A. Yamada, "Multi-Subregion-Based Probabilistic Approach toward Pose-Invariant Face Recognition," Proc. IEEE Int'l Symp. Computational Intelligence in Robotics and Automation, pp. 954-959, 2003

[28] O. Aghazadeh and S. Carlsson. Properties of Datasets Predict the Performance of Classifiers, Proc. British Machine Vision Conference (BMVC), pp. 44.1-44.10, 2013.

[29] J. P. Lewis, "Fast normalized cross-correlation." Vision interface. Vol. 10. No. 1. 1995.

[30] K.C. Lee and J. Ho and D. Kriegman, Acquiring Linear Subspaces for Face Recognition under Variable Lighting, IEEE Trans. Pattern Anal. Mach. Intelligence. 27 (5) (2005) 684–698

[31] M. Turk and A. Pentland, "Face recognition using eigenfaces," IEEE Conference on Computer Vision andPattern Recognition, CVPR, 1991.

[32] F. Zhong, "L1-norm-based (2D)^2PCA," Conference on Computer Science and Electrical Engineering, pp. 1293-1296, 2013.

[33] T. Shakunaga and K. Shigenari, "Decomposed eigen face for face recognition under various lighting conditions," Proceedings of the 2001 IEEE Conference on Computer Vision and Pattern Recognition, CVPR, 2001.

[34] P. Belhumeur, J. Hespanha and D. Kriegman, "Eig faces vs. fisherfaces: Recognition using class specific linear projection," IEEE Transactions on Pattern Analysis and Machine Intelligence, PAMI, pp. 711-720, 1997.

[35] P.N. Belhumeur, J.P. Hespanha, D.J. Kriegman, Eigenfaces vs. Fisherface: recognition using class specific linear projection, IEEE Trans. Pattern Anal. Mach. Intell. 19 (7) (1997) 711–720.

[36] N. Kwak, J. Oh, Feature extraction for one-class classification problems: enhancements to biased discriminant analysis, Pattern Recognition 42 (2009) 17–26.

[37] Z.Z. Liang, Y.F. Li, P.F. Shi, A note on two-dimensional linear discriminant analysis, Pattern Recognition Letters 29 (2008) 2122–2128.

[38] L. Rueda, M. Herrera, Linear dimensionality reduction by maximizing the Chernoff distance in the transformed space, Pattern Recognition 41 (2008) 3138–3152.

[39] Y. Yan, Y.J. Zhang, A novel class-dependence feature analysis method for face recognition, Pattern Recognition Letters 29 (2008) 1907–1914.

[40] C. Cortes and V. Vapnik, "Support-vector networks," Machine learning, vol. 20, pp. 273-297, 1995.

[41] C.W. Hsu and C.J. Lin. A comparison of methods for multiclass support vector machins. IEEE Transactions on Neural Networks, 13(2), March 2002.

[42] Theil, H., Economic forecasts and policy. 1958.

[43] Gayawan, Ezra, and Reuben A. Ipinyomi. "A Comparison of Akaike, Schwarz and R Square Criteria for Model Selection Using Some Fertility Models. "Australian Journal of Basic and Applied Sciences 3.4 (2009): 3524-3530.

ACCEPTED MANUSCRIPT

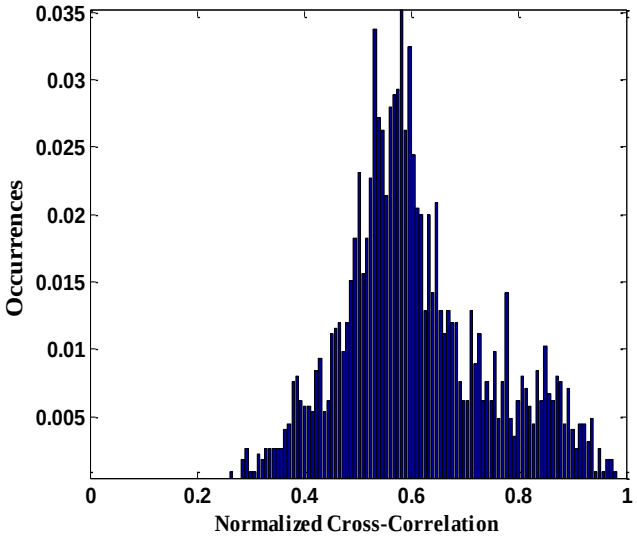

(a)

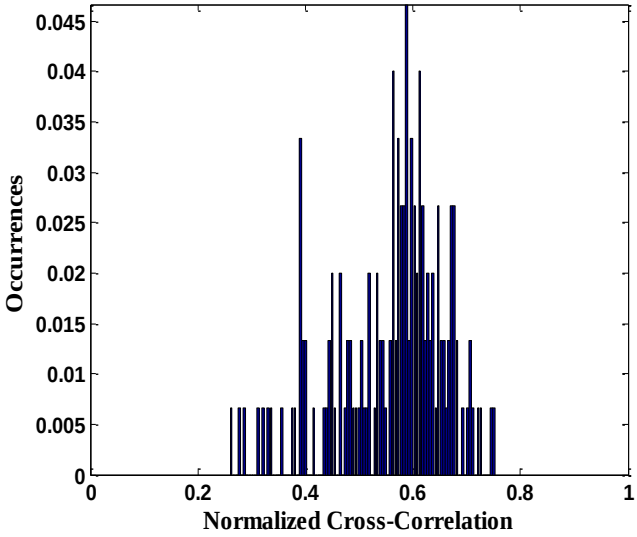

(b)

Fig.1: Normalized Histogram; a) is based on $\hat{\mathbf{C}}_1$ NCC values obtained from a dataset with 10 images per subject which correspond to relatively small change in pose along the 0^o from to 180^o range. b) is based on set $\hat{\mathbf{C}}_2$ NCC values obtained from a dataset with only three images per person representing pose rotations 0^o, 90^o and 180^o.

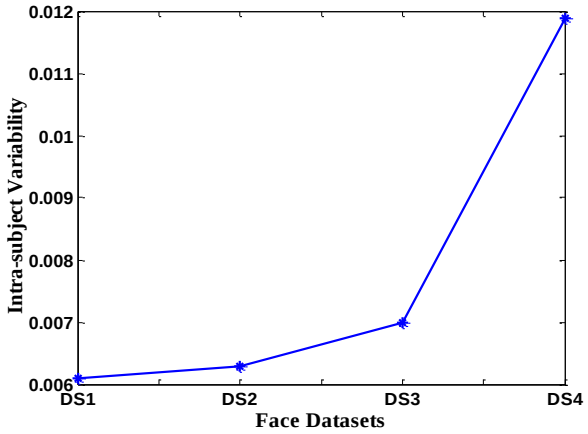

Fig.2: Four face datasets are shown on x-axis. DS1 contains 3 images per subject with a 90^o pose variation between successive images, whereas DS4 has 10 images per subject and the least pose variation across images. i.e. approximately 22.5^o.

Fig.3: Examples of manually cropped images and their corresponding original images.

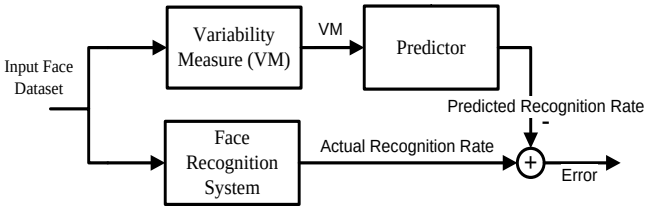

Fig.4: Experimental framework for evaluating prediction error ranges.

ACCEPTED MANUSCRIPT

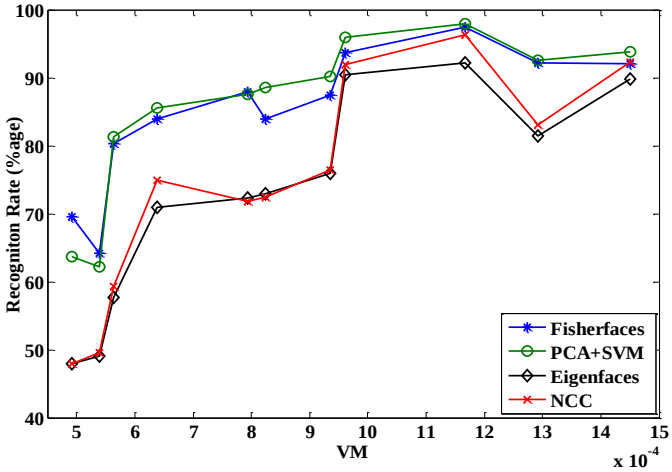

Fig.5: Recognition Rate Vs VM values obtained from 11 datasets and for four different FR systems

ACCEPTED MANUSCRIPT

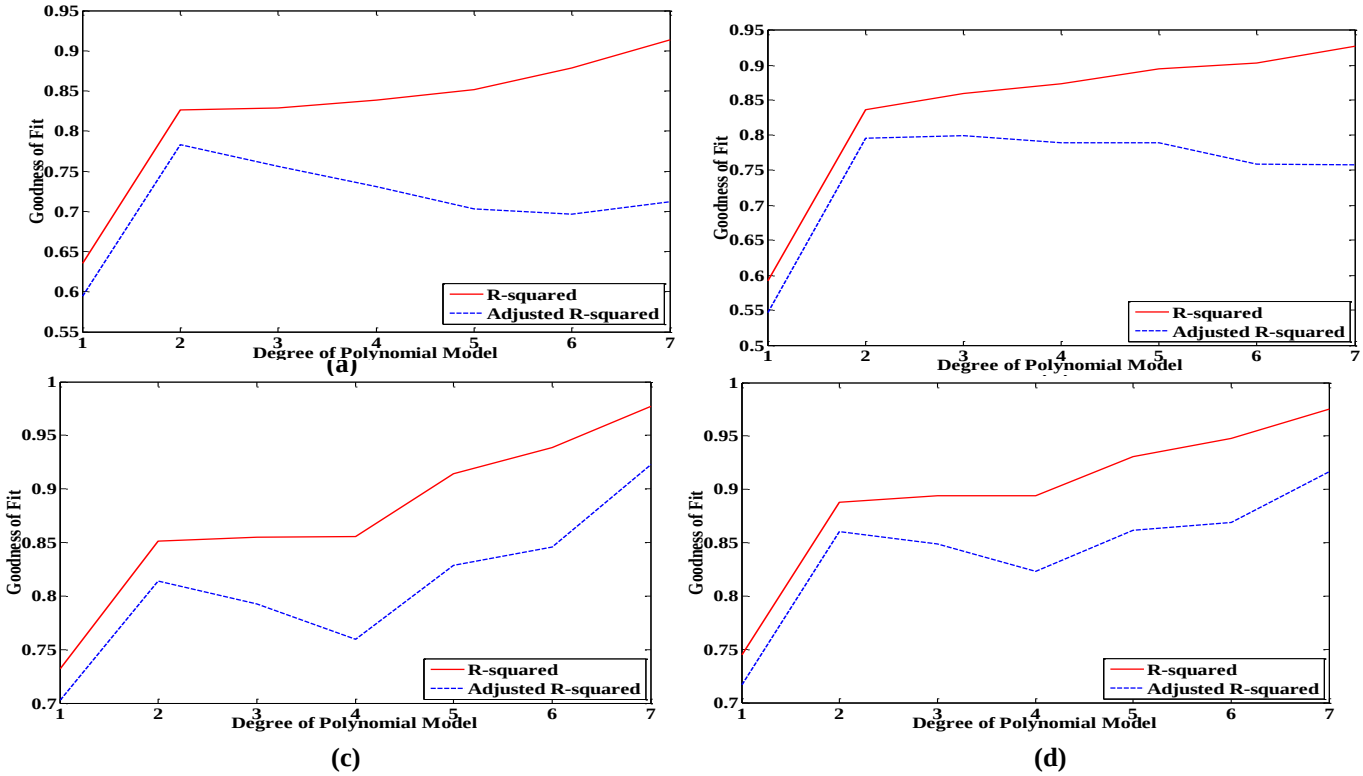

Fig.6: R^2 and $\overline{R^2}$ Vs degree of Polynomial; a) Fisherfaces, b) PCA+SVM, c) Eigenfaces, and d) NCC.

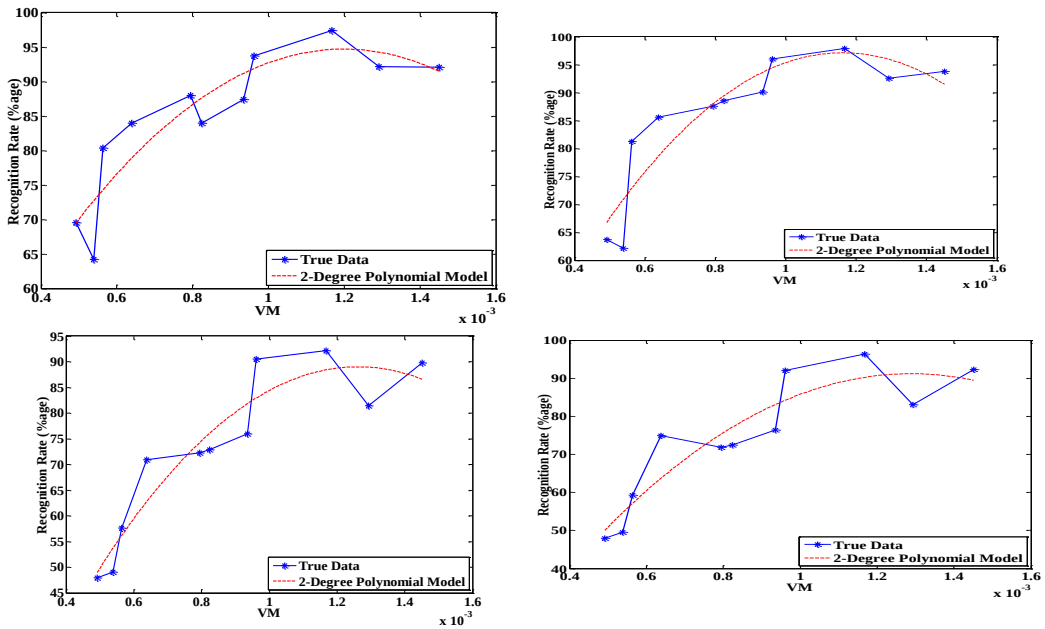

Fig.7: Recognition Rate Vs VM values for a) Fisherfaces, b) PCA+SVM, c) Eigenfaces, and d) NCC. 2nd degree polynomial models shown as dotted lines.

ACCEPTED MANUSCRIPT

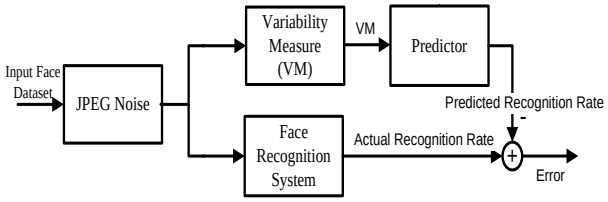

Fig.8: Experimental framework for evaluating proposed VM using noisy data.

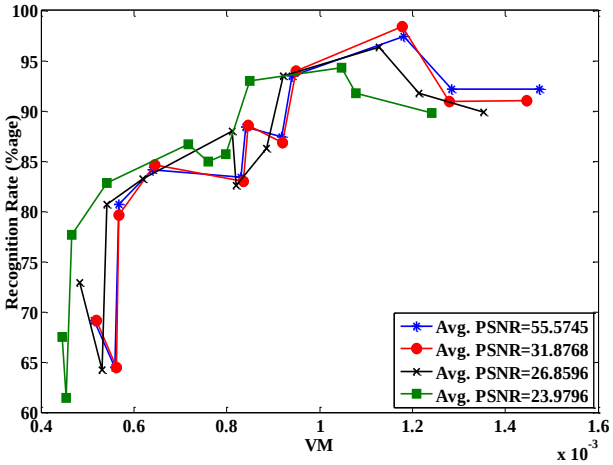

Fig.9: FRSP/VM curves corresponding to Fisherfaces FR system: same overall increasing trend as seen in Fig.5 can also be noticed in case of noise with all PSNR values.

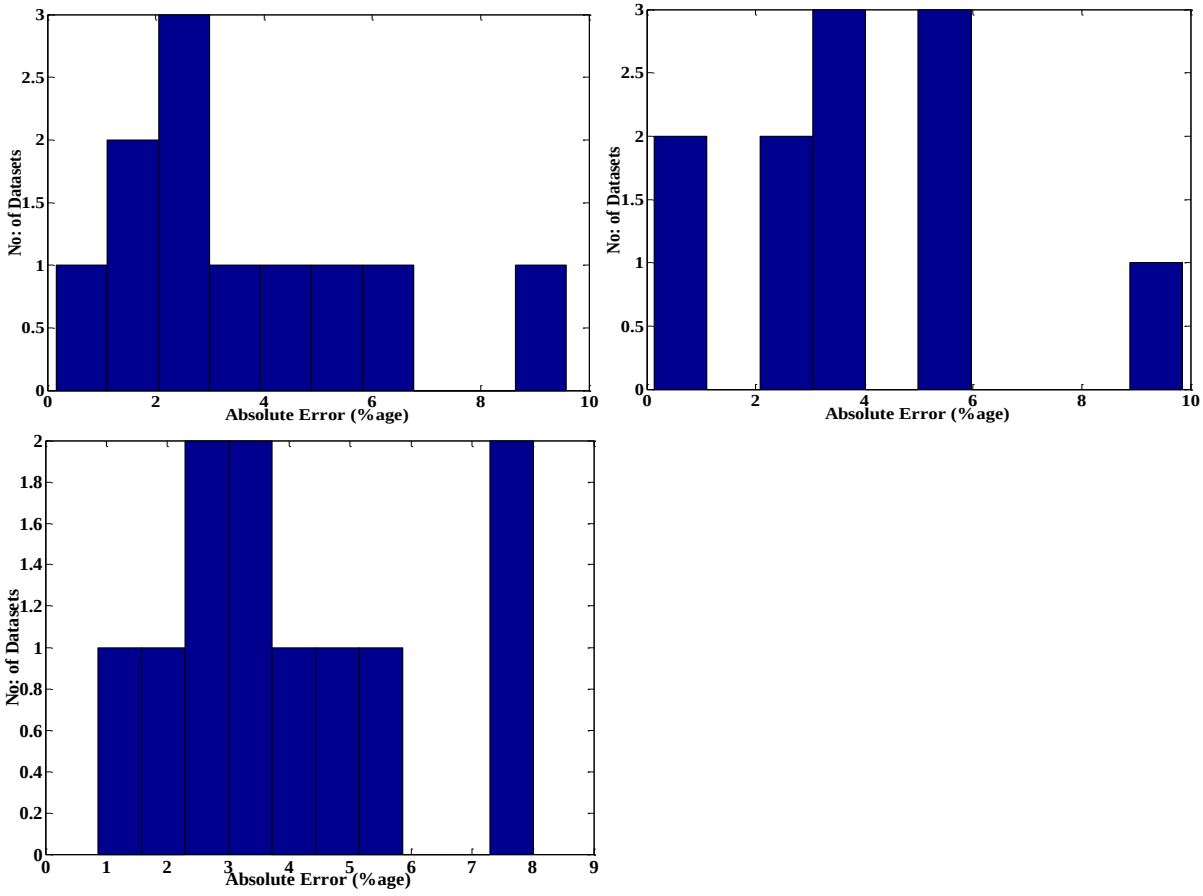

ACCEPTED MANUSCRIPT

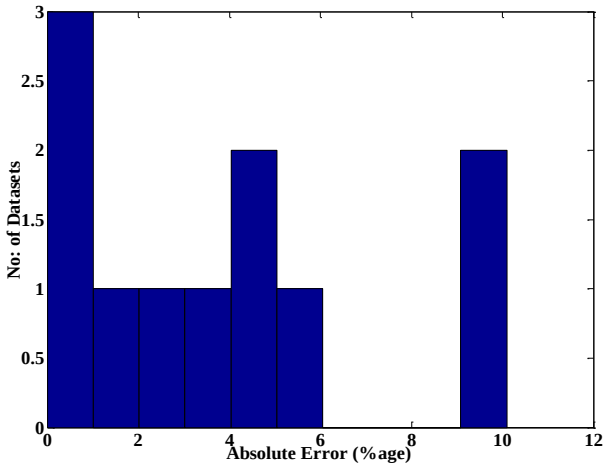

Fig.10: Histograms of Absolute Errors calculated using i) datasets corrupted by JPEG noise at four different PSNR values: a) 55.57, b) 33.48, c) 26.86, and d) 23.98. and ii) FRSP/VM models derived from clean data.

ACCEPTED MANUSCRIPT

Table 1: Some of the widely used Face Datasets in Face Recognition Applications

Database	RGB/Gray	Image Size	No: of Subjects	No: of Images / Subject	Variation
AT&T Face Dataset [10]	Gray	112x92	40	10	Pose, Illumination, expression
IMM Face Dataset [11]	RGB/Gray	640x480	40	6	Pose, Illumination, expression
The Extended Yale Face Dataset [12]	Gray	168x192	28	~576	Illumination, pose
Georgia Tech. Face Dataset [13]	RGB	640x480	50	15	Pose, Illumination, expression
Stirling Face Dataset [14]	Gray	269x369	35	9	Pose, expression
Indian Face Dataset [15]	RGB	640x480	61	11	Pose, Illumination, expression
FEI Face Dataset [16]	RGB	640x480	200	14	Pose, Illumination, expression
XM2VTSDB [17]	RGB	576x720	295		Pose
UMIST Face Dataset [18]	Gray	220x220	20	19-36	Pose

Table 2: Face Datasets having Pose Variation

Database	No: of Subjects	Pose Variation
AT&T Face Dataset [10]	40	10 random poses within ±20 in Yaw and Tilt
Bern Uni Face Dataset [19]	30	5 poses: 0^o, ±20 in Yaw and Tilt
XM2VTSDB [17]	125	5 poses: 0^o, ±30 in Yaw and Tilt
WVU [20]	40	7 poses: 0^o, ±20, ±40, ±60 in Yaw
MIT Face Dataset [21]	62	10 random poses within ±40 in Yaw and Tilt
Asian Face Dataset [22]	46	5 poses: 0^o, ±20, ±25 in Yaw

ACCEPTED MANUSCRIPT

Table 3: Recognition Rate reported for different Pose Variation

Database	No: of Subjects	Pose Difference among Images	Reported Recognition Rate
FERET [24]	100	22.5º / 67.5º / 90º	100 / 99 / 92 [23]
CMU PIE [25]	68	16º / 45º	99.85 / 89.7 [26]
CMU PIE [25]	34	45º / 67.5º / 90º	100 / 80 / 40 [27]

Table 4: Parameters for 2nd-degree Polynomial Model

FR Systems	R^2	$\overline{R^2}$	Avg. AE (%age)	Error Range (%age)
Fisherfaces	0.827	0.783	3.27	0.13-8.5
PCA+SVM	0.837	0.796	3.63	0.41-8.7
Eigenfaces	0.889	0.860	4.40	1.08-8.1
NCC	0.8510	0.814	5.47	2.08-11.1

Table 5: Avg. Absolute Error (Avg. AE) at different Avg. PSNR values.

Avg. PSNR	Avg. AE (%age)	Error Range (%age)
55.57	3.54	0.17-9.59
33.48	3.82	0.13-9.85
26.86	4.16	0.86-8.01
23.98	3.95	0.001-10.9

Appendix-A

Fisherfaces:-

$$y = p_1x^2 + p_2x + p_3 \quad \text{(A-1)}$$

x is normalized by mean 0.000878 and std 0.0003201.
Coefficients (with 95% confidence bounds).
$p_1 = -5.188\ (-9.211, -1.165)$
$p_2 = 10.38\ (6.5, 14.25)$
$p_3 = 89.53\ (84.6, 94.46)$

PCA+SVM:-

$$y = p_1x^2 + p_2x + p_3 \quad \text{(A-2)}$$

x is normalized by mean 0.000878 and std 0.0003201.
Coefficients (with 95% confidence bounds).
$p_1 = -6.926\ (-11.54, -2.31)$
$p_2 = 12.28\ (7.827, 16.72)$
$p_3 = 91.69\ (86.04, 97.35)$

Eigenfaces:-

$$y = p_1x^2 + p_2x + p_3 \quad \text{(A-3)}$$

x is normalized by mean 0.000878 and std 0.0003201.
Coefficients (with 95% confidence bounds).
$p_1 = -6.919\ (-11.9, -1.933)$
$p_2 = 16.58\ (11.78, 21.39)$
$p_3 = 79.08\ (72.97, 85.18)$

NCC:-

$$y = p_1x^2 + p_2x + p_3 \quad \text{(A-4)}$$

x is normalized by mean 0.000878 and std 0.0003201.
Coefficients (with 95% confidence bounds).
$p_1 = -6.632\ (-12.69, -0.5738)$
$p_2 = 17.05\ (11.21, 22.89)$
$p_3 = 80.23\ (72.81, 87.65)$

Note:- These models have been created using MATLAB R20011b simulations.